LXR directly regulates glycosphingolipid synthesis and affects human CD4+ T cell function

Kirsty E. Waddington[a,b,1], George A. Robinson[a], Beatriz Rubio-Cuesta[b,2], Eden Chrifi-Alaoui[a], Sara Andreone[a,3], Kok-Siong Poon[b,4], Iveta Ivanova[c], Lucia Martin-Gutierrez[a], Dylan M. Owen[c,5], Elizabeth C. Jury[a,6,7], and Inés Pineda-Torra[b,6,7]

[a]Centre for Rheumatology, University College London, London WC1E 6BT, United Kingdom; [b]Centre for Cardiometabolic and Vascular Science, University College London, London WC1E 6BT, United Kingdom; and [c]Department of Physics, Randall Division of Cell and Molecular Biophysics, King's College London, London WC2R 2LS, United Kingdom

Edited by Peter Tontonoz, University of California, Los Angeles, CA, and approved April 5, 2021 (received for review September 2, 2020)

The liver X receptor (LXR) is a key transcriptional regulator of cholesterol, fatty acid, and phospholipid metabolism. Dynamic remodeling of immunometabolic pathways, including lipid metabolism, is a crucial step in T cell activation. Here, we explored the role of LXR-regulated metabolic processes in primary human CD4$^+$ T cells and their role in controlling plasma membrane lipids (glycosphingolipids and cholesterol), which strongly influence T cell immune signaling and function. Crucially, we identified the glycosphingolipid biosynthesis enzyme glucosylceramide synthase as a direct transcriptional LXR target. LXR activation by agonist GW3965 or endogenous oxysterol ligands significantly altered the glycosphingolipid:cholesterol balance in the plasma membrane by increasing glycosphingolipid levels and reducing cholesterol. Consequently, LXR activation lowered plasma membrane lipid order (stability), and an LXR antagonist could block this effect. LXR stimulation also reduced lipid order at the immune synapse and accelerated activation of proximal T cell signaling molecules. Ultimately, LXR activation dampened proinflammatory T cell function. Finally, compared with responder T cells, regulatory T cells had a distinct pattern of LXR target gene expression corresponding to reduced lipid order. This suggests LXR-driven lipid metabolism could contribute to functional specialization of these T cell subsets. Overall, we report a mode of action for LXR in T cells involving the regulation of glycosphingolipid and cholesterol metabolism and demonstrate its relevance in modulating T cell function.

LXR | CD4$^+$ T cells | glycosphingolipids | cholesterol | lipid metabolism

CD4$^+$ T cells (also known as T helper cells) shape the immune response by releasing cytokines with both proinflammatory and immunomodulatory effects. A number of factors govern the precise balance of pro- and antiinflammatory mediators produced, including antigenic stimulation, cell–cell signaling, and microenvironmental cues. The T cell plasma membrane facilitates these processes, providing a flexible interface between the cell and its microenvironment in which membrane receptors integrate internal and external signals to generate functional outcomes. Lipids are a key component of the plasma membrane and contribute to its biophysical properties and protein receptor compartmentalization. Cholesterol and glycosphingolipids are particularly enriched, forming signaling platforms known as lipid rafts which play a critical role in T cell antigen receptor (TCR) signaling and T cell function (1). Cholesterol maintains lipid raft structure, inhibits spontaneous TCR activation, and promotes TCR clustering (2, 3). In addition, cholesterol has been shown to regulate T cell proliferation (4, 5), differentiation, and cytokine production (6). Similarly, glycosphingolipids influence TCR-mediated signaling, responsiveness to cytokine stimulation, and T_H17 cell differentiation (7, 8). Plasma membrane cholesterol and glycosphingolipid levels influence lipid order, a measure of how tightly packed lipids are in the membrane (9); notably increased cholesterol is associated with higher lipid order (9–11). Variations in lipid order can influence the interaction of membrane receptors and determine the strength of cell signaling (12). In particular, changes in lipid order at the T cell immune synapse can alter the strength and nature of signaling events and impact T cell function (9, 10, 13). Importantly, abnormal T cell plasma membrane lipids have been linked to pathogenic T cell function and are attractive targets for immunotherapy in autoimmunity, viral infection, and cancer (14–19).

Our previous work linked pathogenic elevation of CD4$^+$ T cell glycosphingolipid expression in systemic lupus erythematosus (SLE) to liver X receptor (LXR) expression (7). LXRα (*NR1H3*) and LXRβ (*NR1H2*) are transcription factors activated by oxidized derivatives of cholesterol (oxysterols) (20) and intermediates of cholesterol biosynthesis (20) to regulate gene expression. The majority of LXR target genes are involved in the metabolism of lipid metabolic processes, including cholesterol efflux and uptake, fatty acid biosynthesis, and phospholipid remodeling (20). However, it is not known whether LXR regulates glycosphingolipid

Significance

This work shows that the liver X receptor (LXR) regulates glycosphingolipid biosynthesis expression in primary human T cells, thereby influencing T cell plasma membrane lipid composition, subsequent immune synapse formation, and T cell receptor-mediated signaling and function. Furthermore, we show LXR actions are differentially regulated in functional T cell subsets, supporting an important role for lipid metabolism in human T cell homeostasis. This new mode of action for LXR could be of therapeutic relevance to disorders characterized by defects in T cell signaling and metabolism, including autoimmune and neurodegenerative diseases, cardiovascular disease, and cancer.

Author contributions: K.E.W., E.C.J., and I.P.-T. designed research; K.E.W., G.A.R., B.R.-C., E.C.-A., S.A., K.-S.P., I.I., and L.M.-G. performed research; K.E.W., G.A.R., B.R.-C., E.C.-A., S.A., K.-S.P., I.I., L.M.-G., D.M.O., E.C.J., and I.P.-T. analyzed data; and K.E.W., E.C.J., and I.P.-T. wrote the paper.

The authors declare no competing interest.

This article is a PNAS Direct Submission.

[1]Present address: Research Biology, GammaDelta Therapeutics Limited, London W12 7FQ, United Kingdom.

[2]Present address: Translational Oncology Laboratory, Research Institute i+12, Spanish National Cancer Research Centre, Universidad Autonoma de Madrid, 28029 Madrid, Spain.

[3]Present address: Department of Oncology and Molecular Medicine, Istituto Superiore di Sanità, 00161 Roma, Italy.

[4]Present address: Department of Pathology, Yong Loo Lin School of Medicine, National University of Singapore, Singapore 119077.

[5]Present address: Department of Mathematics, Institute of Immunology and Immunotherapy, and Centre for Membrane Proteins and Receptors, University of Birmingham, Birmingham B15 2TT, United Kingdom.

[6]E.C.J. and I.P.-T. contributed equally to this work.

[7]To whom correspondence may be addressed. Email: e.jury@ucl.ac.uk or i.torra@ucl.ac.uk.

This article contains supporting information online at https://www.pnas.org/lookup/suppl/doi:10.1073/pnas.2017394118/-/DCSupplemental.

Published May 18, 2021.

metabolism or T cell lipid rafts. This prompted us to further explore the relationship between LXRs, glycosphingolipid metabolism, and plasma membrane lipid composition.

Here, we demonstrate a role for LXR in human CD4$^+$ T cells that involves modulation of the human T cell transcriptome and lipidome. We show how LXR activation modulates glycosphingolipid and cholesterol homeostasis and define a mechanism for LXR-mediated effects on T cell function via regulation of plasma membrane lipid composition. Finally, we show that regulatory T cells (Tregs) have a distinct plasma membrane lipid profile that corresponds to differential expression of LXR target genes. We propose that regulation of membrane lipids by LXR could contribute to the specialized regulatory functions of this T cell subset.

Results

LXR Transcriptionally Regulates Lipid Metabolic Pathways in Human CD4$^+$ T Cells. To define the transcriptional effects of LXR activation in human CD4$^+$ T cells, primary cells were exposed to the specific LXR agonist GW3965 (GW) (21). In total, 65 LXR-responsive genes were identified (Fig. 1 *A* and *B*, Dataset S1) (22), and GW-treated samples were clearly distinguishable from their controls by principal component analysis (*SI Appendix*, Fig. S1*A*). The majority of differentially expressed genes (DEGs) were up-regulated (53 out of 65), a subset of which demonstrated a very strong ligand response. These included well-characterized LXR target genes [*ABCG1*, *ABCA1*, *APOC1*, *SCD*, and *SREBF1* (23)] and the recently identified oligodendrocyte maturation-associated long intervening noncoding RNA (*OLMALINC*) (24) (Fig. 1*C* and *SI Appendix*, Fig. S1*B*). Other previously identified LXR target genes had a more modest up-regulation (less than fivefold) (*SI Appendix*, Fig. S1*C*). The significantly enriched pathways were hierarchically clustered into functionally related groups (Fig. 1*D*). Strikingly, all 15 clusters enriched for LXR–up-regulated genes were related to metabolism, the most significant of which was "cholesterol metabolic process." Only 12 genes were significantly down-regulated by GW (Fig. 1 *A* and *B* and *SI Appendix*, Fig. S1*B*), and these were most strongly associated with the "regulation of inflammatory responses" (Fig. 1*E*).

LXRs can act in a subtype-specific manner, and the relative expression of LXRα and β differs between monocytes/macrophages and T cells (4, 25) (*SI Appendix*, Fig. S1 *D* and *E*). Another striking difference is that in monocytes/macrophages, LXRα regulates its own expression via an autoregulatory loop (26) which does not occur in T cells (*SI Appendix*, Fig. S1*F*). These differences likely lead to cell type–specific responses to LXR activation. To identify potential T cell–specific LXR targets, we cross-referenced our list of DEGs with two publicly available RNA-sequencing (RNA-seq) datasets from murine macrophages (mMφ) treated with GW (27, 28). Of the DEGs identified in T cells, 52% were similarly regulated in mMφ, and remarkably, 29% were uniquely regulated in the T cell dataset (Fig. 1*F*). Some of these genes are known to be differentially regulated between mice and humans/primates, but, to our knowledge, a subset has not previously been associated with LXR activation (*BRWD3*, *CHD2*, *MKNK2*, *SLC29A2*, *TDRD6*, *TKT*, and *UGCG*) (*SI Appendix*, Table S1). Overall, genes involved in lipid metabolic pathways were up-regulated in both cell types, but there were no shared pathways among the down-regulated genes, which tended to be involved in the regulation of immunity and inflammation (*SI Appendix*, Fig. S1 *G* and *H*). This supports that the immunomodulatory effects of LXR activation vary between cell types and species (29).

Thus, we have identified genes responsive to LXR activation in human CD4$^+$ T cells, most markedly the up-regulation of genes involved in lipid metabolic processes, and highlighted a subset of genes that may represent human or T cell–specific targets.

LXR Controls Transcriptional Regulation of Glycosphingolipid Biosynthesis Enzyme UGCG. Since LXR activation predominantly regulated genes involved in lipid metabolism, the impact on T cell lipid content was assessed using shotgun lipidomics. Although total intracellular lipid levels were not affected by LXR activation (Fig. 2*A*), 15% of the detected lipid subspecies were significantly regulated (54 out of 366, Fig. 2*B*). Notably, a large proportion of triacylglycerols (TAG) and hexosylceramides (HexCer) were induced by LXR activation, and overall quantities of TAG and HexCer were elevated (Fig. 2 *C*–*E* and *SI Appendix*, Table S5) (30).

LXR regulated many enzymes involved in fatty acid metabolic processes including synthesis, desaturation, and elongation (Fig. 1*D* and Dataset S1). There were no changes in total levels of saturated, monounsaturated, and polyunsaturated lipids. However, among polyunsaturated fatty acids, there was an increase in degree of unsaturation, which is associated with membrane disorder (31, 32) (*SI Appendix*, Fig. S2*A*). Further examination at the lipid class level revealed significant increases in saturated and monounsaturated lipid species, HexCers, and TAG species with more than four double bonds (Fig. 2*C* and *SI Appendix*, Fig.S2*B*).

Thus, this report links LXR activation to HexCer. We observed GW also reduced levels of several ceramides (Fig. 2 *B* and *C*), suggesting an accelerated conversion of ceramide to HexCer—a reaction catalyzed by glycosphingolipid biosynthesis enzymes UDP-glucosylceramide synthase (UGCG) or UDP-glycosyltransferase 8 (UGT8) (Fig. 2 *F* and *G*). In support of this, UGCG messenger RNA (mRNA) expression was up-regulated by LXR activation (Fig. 2*H*), whereas UGT8 was absent in CD4$^+$ T cells (*SI Appendix*, Fig. S2*C*).

UGCG up-regulation was further amplified by costimulation of LXR and its heterodimeric partner the retinoid X receptor (RXR) (*SI Appendix*, Fig. S2*D*), as has been reported for other LXR target genes (33, 34). GW treatment also enhanced UGCG expression in other immune cell types, including peripheral blood mononuclear cells (PBMCs), CD14$^+$ monocytes, and CD19$^+$ B cells (*SI Appendix*, Fig. S2*E*). However, in monocyte-derived macrophages and THP-1 macrophages, UGCG was only modestly increased (<1.5-fold change, *SI Appendix*, Fig. S2 *E* and *F*). This may explain why UGCG has not been identified as an LXR target gene in previous RNA-seq and chromatin immunoprecipitation (ChIP) sequencing experiments using macrophages (27, 35), in which most of LXR biology has been reported to date. The increase in UGCG expression was not a GW-specific effect, as UGCG mRNA was also up-regulated in response to stimulation with the endogenous LXR activators 24S, 25-epoxycholesterol (24S,25-EC) and 24S-hydroxycholesterol (24S-OHC), albeit with an altered kinetic (*SI Appendix*, Fig. S2*G*).

To determine whether LXR regulates UGCG expression by directly binding to the UGCG locus, we screened for potential LXR response element (LXRE) sequences in silico. A putative DR4 sequence was identified upstream of the UGCG gene that coincided with an LXR-binding peak in HT29 cells treated with GW (36) (*SI Appendix*, Fig. S2*H*). ChIP-qPCR experiments demonstrated enrichment in LXR occupancy at this site, which increased with ligand activation (Fig. 2*I*). The observed LXR occupancy at the UGCG gene followed a similar pattern to that of a reported LXRE within SMPDL3A (37) (Fig. 2*I* and *SI Appendix*, Fig. S2 *H*). Moreover, acetylation of histone H3K27 was enriched at this region compared with the IgG and a negative control sequence, suggesting this site falls in an active transcriptional enhancer (*SI Appendix*, Fig. S2 *I* and *J*).

LXR Regulates the T Cell Plasma Membrane Lipid Raft Profile. UGCG is the rate-limiting enzyme for the biosynthesis of glycosphingolipids, important components of plasma membrane lipid rafts. Indeed, LXR activation consistently up-regulated T cell glycosphingolipid expression measured using cholera toxin B (Fig. 3*A*), a well-established surrogate glycosphingolipid marker (7). Specific pharmacological inhibition of UGCG activity blocked the induction of glycosphingolipids by GW, suggesting

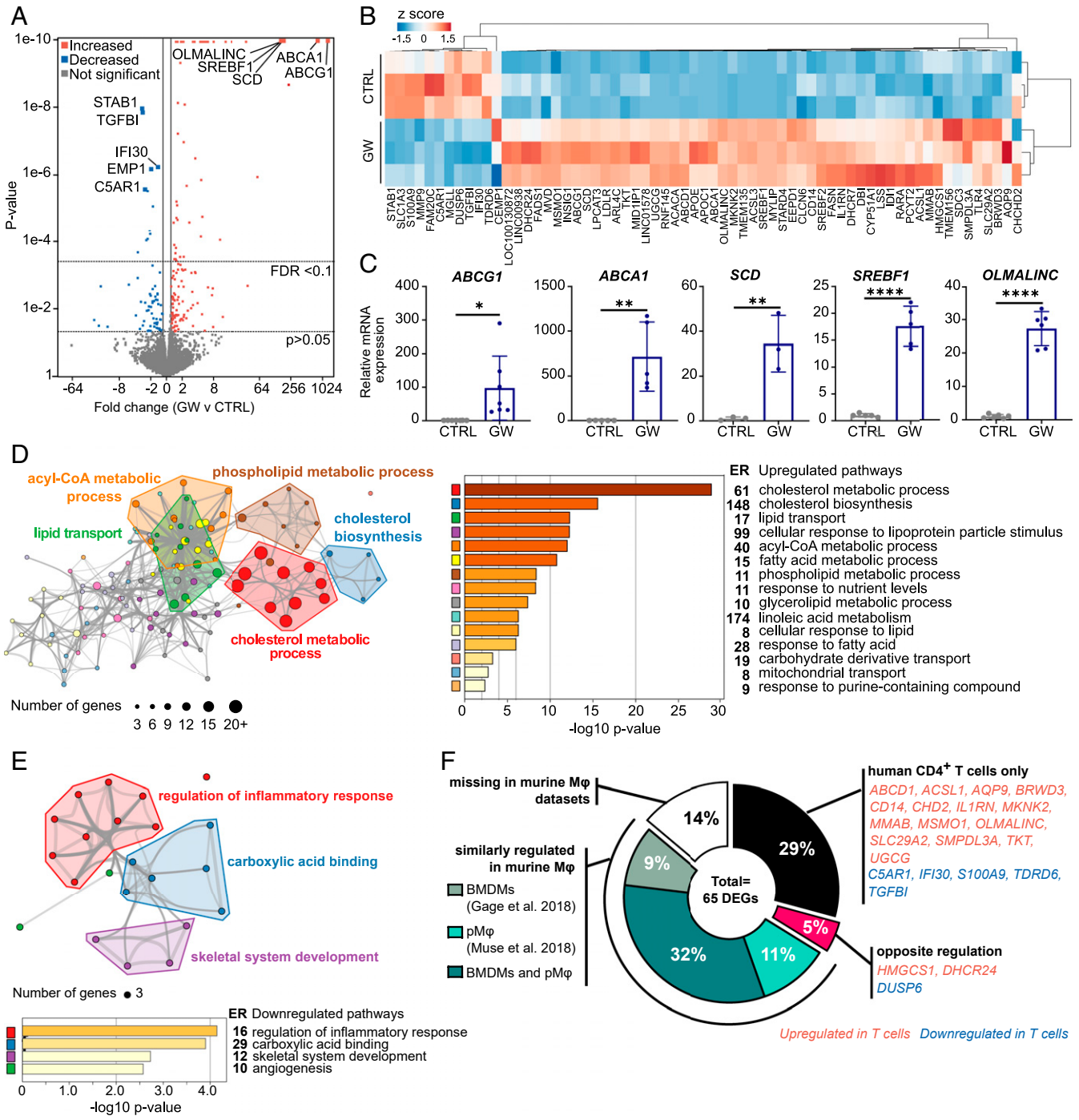

Fig. 1. LXR regulates lipid metabolism in human CD4+ T cells. Primary human CD4+ T cells ($n = 3$) were cultured with or without LXR agonist (GW3965, GW) for 24 h. Gene expression was assessed by RNA-seq. (*A*) Volcano plot showing fold changes and *P* values. Colored points represent significantly regulated genes ($P < 0.05$). (*B*) Clustered heatmap of normalized gene counts of all LXR-regulated genes with FDR-corrected $P < 0.1$. (*C*) Regulation of a selection of genes was confirmed by qPCR in an independent set of donors ($n = 3$ to 6). Bars represent mean ± SD. Unpaired two-tailed *t* test; $*P < 0.05$, $**P < 0.01$, $****P < 0.0001$. (*D* and *E*) Network diagrams illustrate pathways significantly enriched for up- (*D*) or down- (*E*) regulated genes. Each node represents a significantly enriched term, with node size proportional to the number of contributing genes. Similar terms with a high degree of redundancy were clustered, as depicted. Bar charts plot cluster significance and show enrichment ratios (ER). (*F*) Pie chart showing the proportion of genes regulated by GW in human T cells that are also regulated in murine bone marrow–derived macrophages (BMDMs) (21) or peritoneal macrophages (pMφ) (23).

this was UGCG dependent (*SI Appendix*, Fig. S2*K*). The increase in glycosphingolipid levels was accompanied by significant down-regulation of membrane cholesterol (Fig. 3*B*), likely due to the strong induction of cholesterol efflux transporters ABCA1 and ABCG1 (Fig. 1*C* and *SI Appendix*, Fig. S2*M*). As expected, UGCG inhibition had no effect on the reduction of cholesterol or lipid order (*SI Appendix*, Fig. S2*K*). Overall, LXR activation significantly increased the ratio of glycosphingolipids to cholesterol (Fig. 3*C*).

The relative abundance and arrangement of lipids in the plasma membrane dictates its "lipid order," an important determinant of signaling protein localization during immune synapse formation

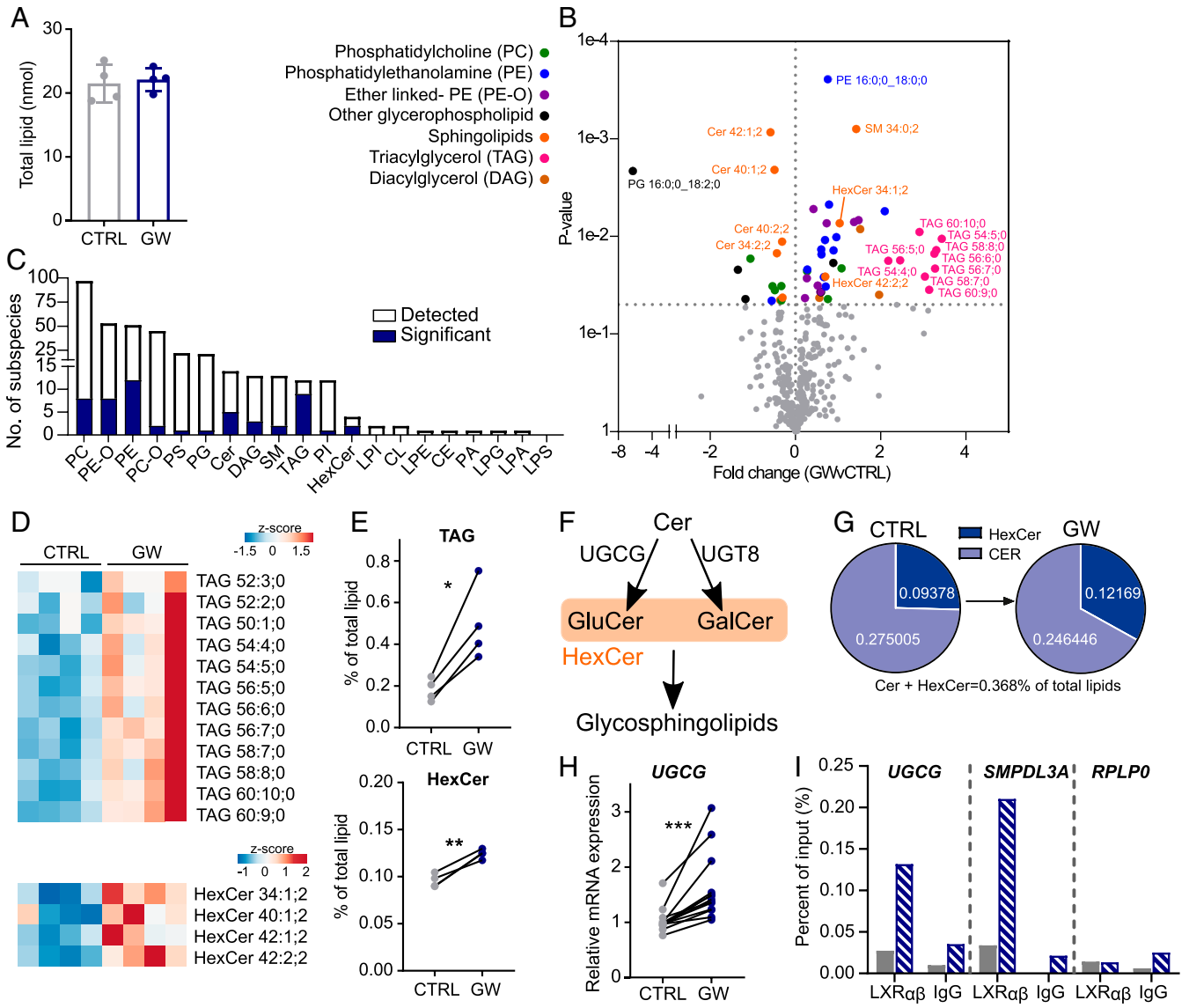

Fig. 2. LXR activation regulates the transcription of UGCG. (*A–E*) Primary human CD3$^+$ T cells ($n = 4$) were sorted by FACS and treated ± GW (2 μM) for 36 h and total cellular lipid content analyzed by shotgun lipidomics. (*A*) Total lipids (normalized to cell numbers) were unchanged (mean ± SD). (*B*) Volcano plot represents significant changes in the expression of lipid subspecies, color-coded by broader lipid class ($P < 0.05$). (*C*) Bars show the number of subspecies detected for each lipid type. The filled area represents the proportion of subspecies significantly altered by GW treatment. (*D*) Unclustered heatmaps represent levels of individual subspecies. (*E*) Dot plots show overall change in TAG and HexCer levels. (*F*) Schematic illustrating the role of UGCG in the conversion of ceramide to HexCer. (*G*) Pie chart showing a GW-induced shift from Cer to HexCer. (*H*) Up-regulation of UGCG mRNA expression in CD4$^+$ T cells after 24 h GW treatment ($n = 13$). (*I*) Cells were treated with DMSO (gray bars), LXR (GW, 1 μM), and RXR (LG100268; LG, 100 nM) ligands (hatched bars) for 2 h. LXR occupancy at the putative DR4 motif at *UGCG* compared with IgG control, positive control (*SMPDL3A*), and negative control (*RPLP0*) sequences. Representative of three independent experiments. (*A–H*) Two-tailed *t* tests: $^*P < 0.05$, $^{**}P < 0.01$, $^{***}P < 0.001$. Abbreviations: Cer, ceramide; PE, phosphatidylethanolamine; DAG, diacylglycerol; HexCer, hexosylceramide; SM, sphingomyelin; PE-O, phosphatidylethanolamine-ether; PI, phosphatidylinositol; PC, phosphatidylcholine; PS, phosphatidylserine; PC-O, phosphatidylcholine-ether; LPI, lyso-phosphotidylinositol; LPE, lyso-phosphatidylethanolamine; CE, cholesterol esters; PA, phosphatidate; CL, cardiolipin; LPG, lyso-phosphatidylglycerol; LPA, lyso-phosphatidate; and LPS, lyso-phosphatidylserine.

(10). Cholesterol levels positively correlate with T cell plasma membrane lipid order, whereas glycosphingolipid levels have a negative correlation (9). LXR lowers cholesterol and raises glycosphingolipids, resulting in the significant reduction of membrane lipid order by GW-/oxysterol-activated LXR (Fig. 3 *D* and *E* and *SI Appendix*, Fig. S2 *K* and *L*). The specific LXR antagonist GSK233 was able to block the reduction of lipid order, glycosphingolipid, and cholesterol levels by GW (Fig. 3*E* and *SI Appendix*, Fig. S2*L*). Oxysterols also activated LXR target gene expression and reduced lipid order while GSK233 only partially reversed the effect of 24S-OHC, in line with the known LXR-independent actions of oxysterols (*SI Appendix*, Fig. S2 *M–O*).

Furthermore, LXR target genes were differentially expressed in T cells sorted based on their (high/low) plasma membrane lipid order. T cells with low membrane lipid order (low cholesterol and high glycosphingolipids) had elevated expression of *ABCA1*, *ABCG1*, and *UGCG* compared with T cells with high-membrane lipid order (high cholesterol, low glycosphingolipids) (Fig. 3*F*). This suggests LXR ligand–induced cholesterol efflux (*ABCA1/G1*) and glycosphingolipid biosynthesis (*UGCG*) contribute to the generation of low membrane lipid order. In contrast, there was no

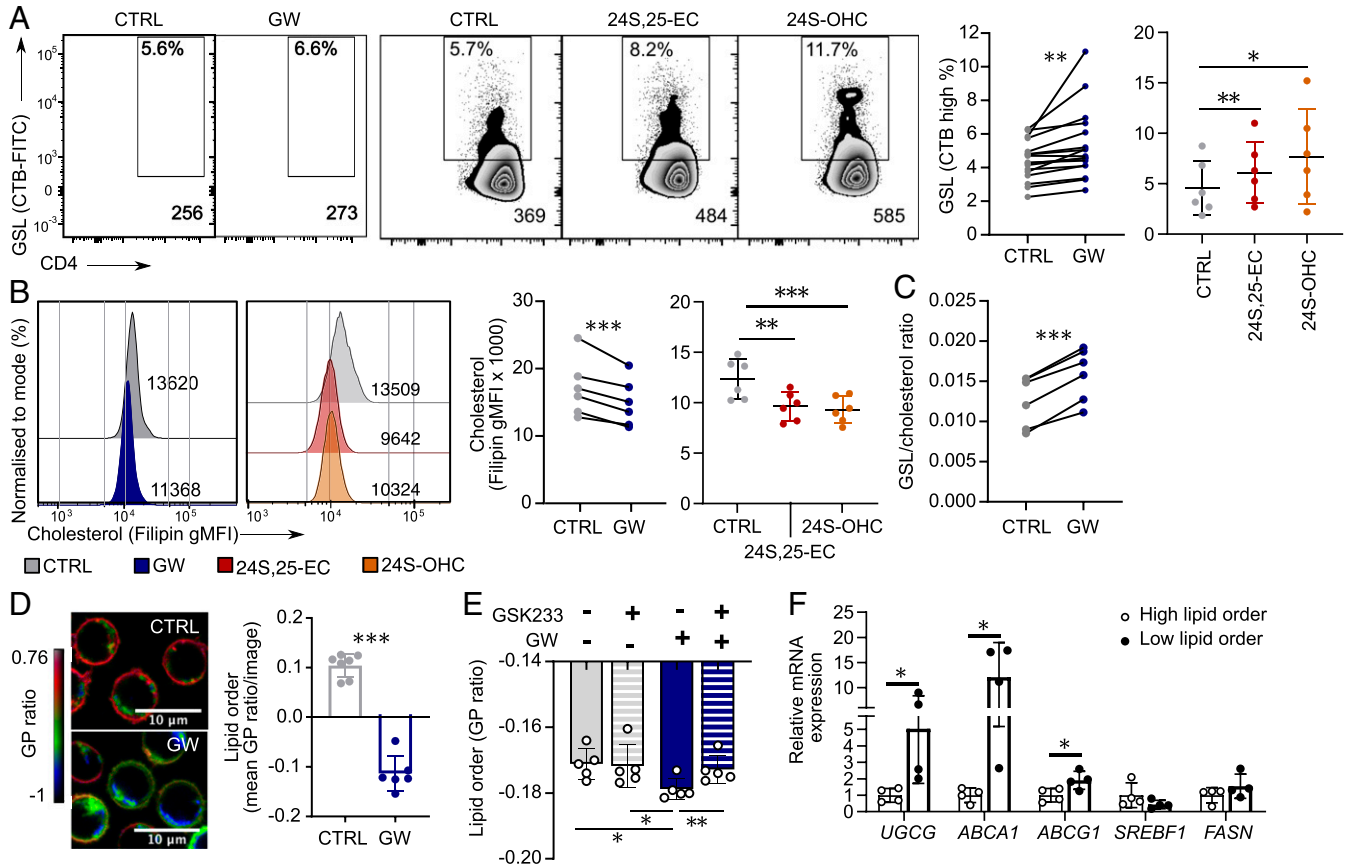

Fig. 3. Plasma membrane lipid order is reduced by LXR activation. (*A–C*) Cells were cultured ± LXR ligands for 24 h (GW) or 72 h (24S,25-EC and 24S-OHC), and flow cytometry was used to identify CD4$^+$ T cells and measure plasma membrane lipid expression in more than four independent experiments. (*A*) Representative flow cytometry plots show the percentage of T cells highly expressing cholera toxin B (CTB) and CTB gMFI as surrogate markers for glycosphingolipids, as in ref. 9. Cumulative data shows change in percentage of cells highly expressing CTB. (*B*) Representative histogram of filipin staining for cholesterol and cumulative data showing change in gMFI. (*C*) Cumulative data showing glycosphingolipid level (GSL)/cholesterol ratio as CTB/filipin ($n = 6$). (*D–F*) Magnetically purified CD4$^+$ T cell membrane lipid order was measured using di-4-ANEPPDHQ. (*D*) Representative confocal microscopy image and a histogram of average GP ratio per image analyzed are shown ($n = 1$ donor). (*E*) Cumulative data from three experiments showing lipid order measured by flow cytometry. Cells were treated with an LXR agonist (GW) or antagonist (GSK233) ($n = 5$) for 24 h. (*F*) di-4-ANEPPDHQ–stained CD4$^+$ T cells ($n = 4$) were sorted into high or low membrane order by FACS, and gene expression was compared by qPCR. Bars show mean ± SD (*A–F*) Two-tailed *t* tests or one-way ANOVA with Tukey's post hoc test; *$P < 0.05$, **$P < 0.01$, ***$P < 0.001$.

difference in the expression of genes controlling fatty acid synthesis (*SREBP1c*, *FASN*) in cells with different membrane order (Fig. 3*F*).

Overall, these data suggest that LXR transcriptionally up-regulates de novo glycosphingolipid synthesis in human T cells, thereby contributing to the remodeling of plasma membrane lipid composition in response to LXR activation.

LXR Activity Modulates Lipid Metabolism and Effector Function of Activated T Cells. Next, we explored the effect of LXR on primary human T cell activation. Over 3,000 genes were significantly regulated by TCR activation, although most of these were regulated irrespective of LXR activation with GW (Fig. 4*A*). Interestingly, LXRβ expression was slightly increased by TCR stimulation, while LXRα expression remained low (*SI Appendix*, Fig. S3*A*). Overall, 113 genes were regulated by the presence or absence of GW in activated T cells (Fig. 4*B*, *SI Appendix*, Fig. S3*B*, and Dataset S2). TCR/LXR costimulation up-regulated genes involved in lipid metabolic processes and down-regulated genes associated with immune system processes including chemokine production and chemotaxis (*SI Appendix*, Fig. S3*C*). When these genes were clustered based on their expression in both activated and resting cells, four major patterns of gene expression were identified (Fig. 4*C* and *SI Appendix*, Table S2). Many genes up-regulated by GW in resting cells were up-regulated to an equal or greater extent in GW/TCR–coactivated cells (clusters A and C, Fig. 4*C*). These clusters were enriched for genes involved in lipid and cholesterol metabolic processes, including canonical LXR target genes *ABCA1* and *SREBF1* and the newly identified LXR target gene *UGCG*. This corresponded with changes in global plasma membrane lipid composition, namely increased glycosphingolipids but reduced cholesterol in response to LXR/TCR costimulation compared with TCR stimulation alone (Fig. 4 *D–F*). Therefore, LXR activation continues to modulate plasma membrane composition throughout the course of T cell activation.

In contrast, GW/TCR costimulation reduced the induction of a subset of genes involved in leukocyte activation (cluster B, Fig. 4*C*). Interestingly, other genes were only activated (cluster C) or repressed (cluster D) by LXR activation in the context of TCR stimulation (Fig. 4*C*). Therefore, bidirectional crosstalk between LXR and TCR stimulation modulates transcription in a gene-specific manner. Likely, more subtle differences did not reach statistical significance due to the heterogeneous response to stimulation between the healthy donors (*SI Appendix*, Fig. S3*D*).

In murine T cells, TCR stimulation was previously reported to repress LXR transcriptional activity by reducing the availability of endogenous LXR ligands due to their modification by the

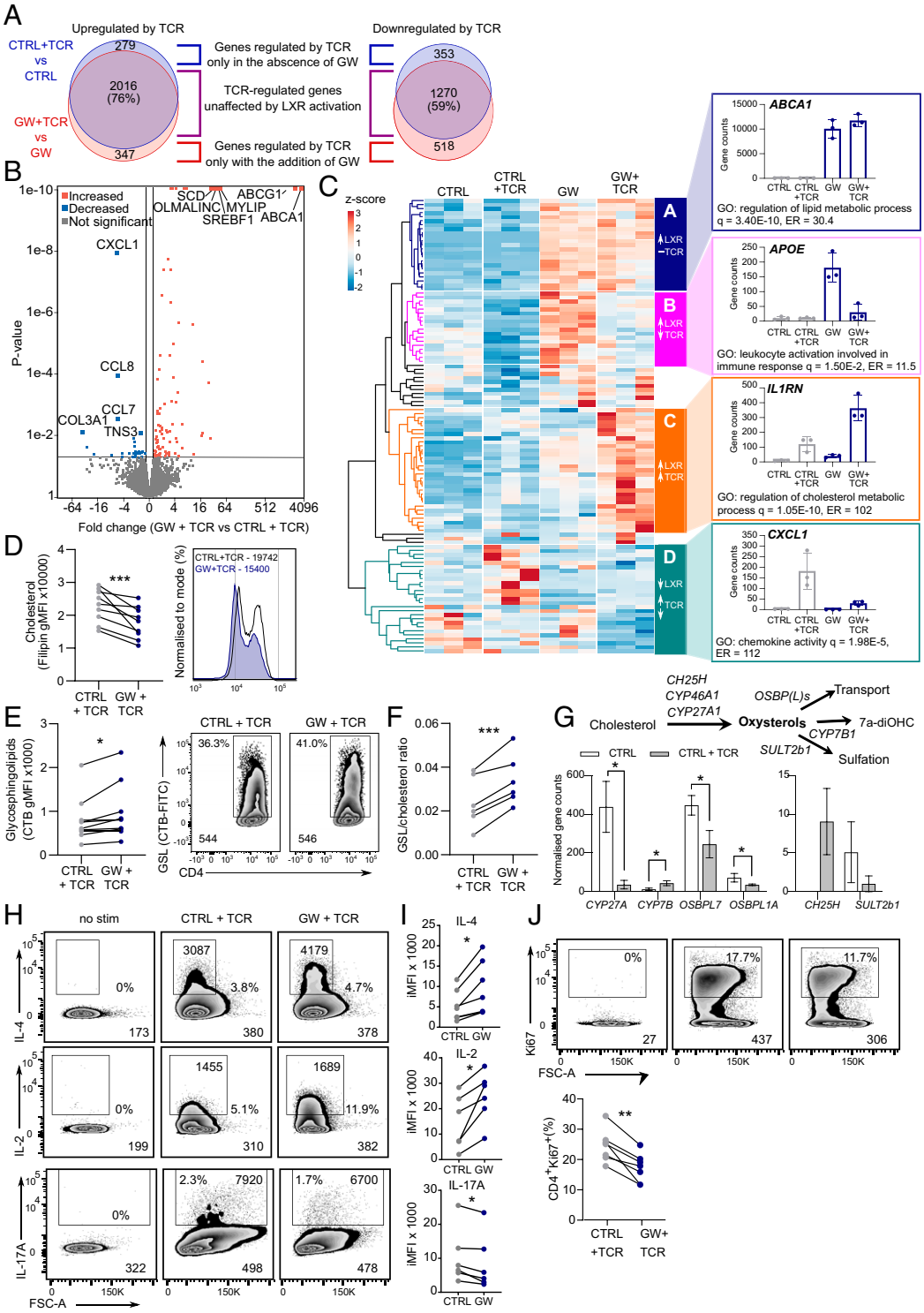

Fig. 4. LXR activation modulates T cell immune function. (*A*–*C*) RNA-seq was performed on magnetically isolated CD4$^+$ T cells incubated ± GW for 6 h before stimulation with anti-CD3/CD28 (TCR) ± GW ($n = 3$). (*A*) Venn diagrams compare the number of genes up- or down-regulated by TCR stimulation in the presence (red) or absence (blue) of GW. (*B*) Volcano plot of genes differentially expressed between GW+TCR and CTRL+TCR. (*C*) Normalized RNA-seq gene counts of differentially expressed genes were compared with resting T cells. Four patterns of gene expression were identified by hierarchical clustering (clusters A through D). One gene from each cluster is shown as an example (mean ± SD), and the most significantly enriched gene ontology (GO) term is given. (*D*–*F*) Representative flow cytometry plots and cumulative data from four independent experiments ($n = 6$ to 9) show the effect of GW on the plasma membrane cholesterol (*D*) and glycosphingolipid (*E*) content of activated CD4$^+$ T cells and the ratio of GSLs to cholesterol (*F*). (*G*) Schematic illustrating enzymes controlling oxysterol metabolism. Bar charts show normalized RNA-seq gene counts of enzymes significantly regulated by TCR activation (mean ± SD, $n = 3$). *FDR < 0.1. (*H*–*J*) Magnetically isolated CD4$^+$ T cells were activated with anti-CD3/CD28 (+TCR) for 72 h in the presence of GW3965 (GW) or control (CTRL). (*H*–*J*) Intracellular cytokines were analyzed by flow cytometry after additional treatment with PMA and ionomycin (*H* and *I*), and Ki67 was used as a marker of proliferation (*J*). Representative flow cytometry plots are labeled with percentage of positive cells and gMFI of both the cytokine-producing/proliferating population and total T cells. Cumulative data from four independent experiments shows cytokine production expressed as an integrated MFI (iMFI = gMFI*frequency of cytokine producing cells (11) (*I*) or percentage of proliferating cells (*J*). Two-tailed *t* tests; *$P < 0.05$, **$P < 0.01$, ***$P < 0.001$.

sulfotransferase SULT2B1 (4). However, in the present study, we observed very low levels of *SULT2B1* in human $CD4^+$ T cells (<11 gene counts), and *SULT2B1* was not regulated by TCR activation (Fig. 4*G*). We considered that oxysterol levels could be controlled by an alternative mechanism, for example increased efflux or metabolism. Indeed, TCR activation down-regulated the expression of oxysterol-binding proteins and oxysterol biosynthesis enzyme *CYP27A1* and up-regulated oxysterol-metabolising enzyme *CYP1B1* (Fig. 4*G*). Therefore, concentrations of endogenous LXR ligands during human T cell activation are also tightly regulated but likely through a different mechanism.

LXR and T cell coactivation had significant functional consequences including increased production of interleukin (IL)-2 and IL-4 and reduced IL-17A release compared with non–LXR-treated controls (Fig. 4 *H* and *I* and *SI Appendix*, Fig. S4 *A* and *B*). No changes in T cell interferon-γ, tumor necrosis factor-α, or IL-10 production were detected (*SI Appendix*, Fig. S4*B*). Although LXR has been reported to regulate the transcription of certain cytokines (6, 38), this was not observed here (Dataset S2). Furthermore, the expression of transcription factors which drive Th1 (Tbet), Th2 (GATA3), Treg (Foxp3), and Th17 (RORγ) polarization were also unaffected by LXR activation (*SI Appendix*, Fig. S4*C*). Proliferation was inhibited by GW treatment (Fig. 4*J* and *SI Appendix*, Fig. S4*D*), and importantly, addition of the UGCG inhibitor NB-DNJ countered this effect by increasing proliferation and partially blocking IL-2 and IL-4 production (*SI Appendix*, Fig. S4 *E* and *F*). Considering the preferential regulation of lipid metabolism genes (*SI Appendix*, Fig. S3*C*) and observed changes in plasma membrane lipid levels (Fig. 4 *D–F*), we instead hypothesized that the effects of LXR activation on T cell function could be mediated, at least in part, by an altered lipid landscape.

LXR-Driven Modification of Plasma Membrane Lipid Profile Alters TCR Signaling. T cell activation is initiated by TCR-proximal signaling at the immune synapse, leading to proliferation and cytokine production. We previously demonstrated that, compared with cells with highly ordered plasma membranes, T cells with lower membrane lipid order have reduced synapse area, transient synapse formation, and a Th1 cytokine skew (9). These functional outcomes are influenced by the localization of TCR signaling proteins within lipid microdomains at the immune synapse (39). To examine the effect of LXR stimulation on the kinetics of lipid reorganization during the early stages of T cell activation, we used di-4-ANEPPDHQ staining and total internal reflection fluorescence (TIRF) microscopy to assess the interaction between $CD4^+$ T cells and antibody-coated glass coverslips (mimicking the "immune synapse") (Fig. 5*A* and Movies S1 and S2). T cells pretreated with GW had a significantly lower membrane order (generalized polarization [GP] ratio) at the cell/coverslip interface for up to 20 min postactivation (Fig. 5*B* and Movies S1 and S2). Synapse area was unaffected (*SI Appendix*, Fig. S4*G*); however, the pattern and distribution of lipid order were disrupted in GW-treated T cells compared with controls (*SI Appendix*, Fig. S4*H*). This was accompanied by increased levels of global tyrosine phosphorylation (Fig. 5*C*), increased accumulation of Lck receptor tyrosine kinase at the synapse (Fig. 5*C*), and a preference for Lck to accumulate at the synapse periphery (Fig. 5*D*), an area typically associated with active signaling (40). Specifically, GW treatment increased phosphorylation of important proximal T cell signaling molecules CD3 and the adaptor molecule linker for activation of T cells (LAT), but not extracellular signal related kinase (Erk) or phospholipase (PL) Cγ1 (*SI Appendix*, Fig. S4*I*).

Taken together, these results suggest that plasticity in T cell function could be driven, at least in part, by altered plasma membrane lipid composition controlled by LXR activation.

Functional T Cell Subsets Differ in Their Expression of LXR-Regulated Genes and Lipids. T cells with high and low membrane lipid order are functionally distinct (9). Compared with responder T cells (Tresp), regulatory T cells (Treg) (Fig. 6*A*) had lower membrane order, increased glycosphingolipid levels, and reduced membrane cholesterol (Fig. 6 *B–D*). We hypothesized that the LXR pathway could contribute to these differences. LXRα mRNA expression was significantly lower in Tregs, although LXRβ, which is the predominant form in T cells (*SI Appendix*, Fig. S1 *D–F*), tended toward higher expression ($P = 0.06$) (Fig. 6*E*). Corresponding to the plasma membrane lipid phenotype, Treg expression of the cholesterol transporter *ABCG1* and glycosphingolipid enzyme *UGCG* were increased compared with Tresp, whereas other LXR target genes were not differentially expressed (*ABCA1*, *IDOL*, *SREBF1*, and *FASN)* (Fig. 6*E*).

Interestingly, Tregs had a more variable response to LXR stimulation than Tresp in terms of reduction of membrane lipid order and induction of glycosphingolipids, although down-regulation of cholesterol was consistently similar (Fig. 6 *F–H*). Mirroring the regulation of glycosphingolipids and cholesterol, cholesterol metabolism genes (*ABCA1*, *ABCG1*, and *IDOL*) were similarly induced in both subsets, whereas UGCG mRNA was significantly up-regulated in Tresp but not Treg (Fig. 6 *G* and *H*). Fatty acid synthesis enzymes had a similar magnitude of regulation (fourfold versus sixfold), although *FASN* levels were much higher in GW-treated Treg than Tresp (Fig. 6*I*).

These results demonstrate that Treg and Tresp have distinct plasma membrane lipid profiles and differences in LXR ligand responses. This suggests that variation in LXR activity could influence the functional specialization of T cell subsets.

Discussion

$CD4^+$ T cells provide essential protection against infection and cancer, but dysregulated T cell responses contribute to the pathogenesis of many diseases. LXRs are an attractive therapeutic target in many immunometabolic diseases involving T cells (41, 42). However, the actions of LXR in lymphocytes have not yet been fully investigated, particularly in human cells. This is important since a number of differences in LXR biology have been reported between human and rodent models, including the aforementioned species-specific regulation of certain genes (24, 26, 37, 43). Furthermore, in stark contrast to the antiinflammatory effects of LXR activation in murine macrophages (44–46), LXR has been shown to potentiate proinflammatory responses in human monocytes (43, 47, 48).

Here, we have comprehensively assessed the action of LXR in human $CD4^+$ T cells, combining transcriptomic and lipidomic analyses with cell biology approaches to study the regulation of lipid metabolism and T cell function. Our findings revealed the regulation of glycosphingolipid biosynthesis by LXR in these cells, which may be replicated in other immune cell types. The combined effect of LXR activation on glycosphingolipid and cholesterol levels contributed to an overall reduction in plasma membrane lipid order, which modulated immune synapse formation and proximal T cell signaling in the context of TCR activation.

While this work was ongoing, LXR was shown to contribute to T cell development in animal models. T cell–specific deletion of LXR resulted in peripheral lymphopenia, thought to be caused by accumulation of plasma membrane cholesterol, heightened apoptotic signaling, and subsequent enhanced negative selection (49). This supports our findings that regulation of plasma membrane lipids by LXR is important for T cell function. Additionally, recent work in murine models highlighted LXRβ's indispensable role in murine Tregs (50). LXR activation was also shown to exert anti-tumor effects by reducing the Treg content of the murine tumor microenvironment (51). While this work stresses the importance of LXR in T cell biology, the impact of LXR on plasma membrane metabolism was not examined.

There is extensive evidence in the literature that UGCG plays an important role in T cell immune synapse formation in vitro and in vivo. Similar to other studies (45), we did not use small interfering RNA-based methods which could adversely influence

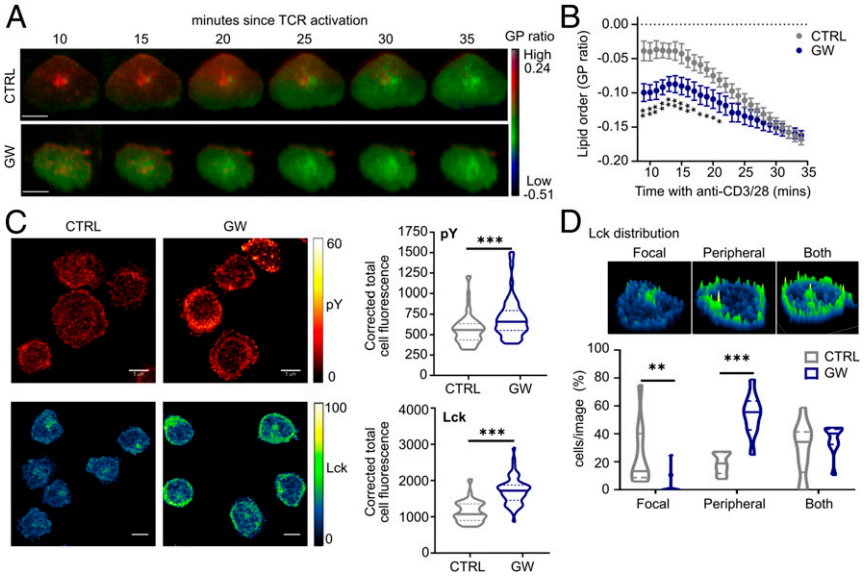

Fig. 5. LXR activation regulates immune synapse formation and proximal TCR signaling. (*A–D*) Magnetically purified CD4$^+$ T cells were cultured ± GW before addition to chamber slides coated with anti-CD3/28 for immune synapse formation. (*A* and *B*) T cells were stained with di-4-ANEPPDHQ, and immune synapse formation was recorded for 30 min using TIRF microscopy. (*A*) Representative images at 5 min intervals. (Scale bar, 5 μM.) (*B*) GP ratio was quantified at each minute (n= 10 to 12 cells/condition, mean ± SEM). (*C* and *D*) Immune synapses ($n = 2$ donors) were fixed at 15 mins post activation and immunostained for Lck (CTRL = 68 cells, GW = 52 cells) and phosphotyrosine (pY) (CTRL = 59 cells, GW = 52 cells). Representative images and quantification of CTCF (*C*) or classification of Lck distribution patterns (*D*). Violin plots show median and quartile values. Multiple unpaired *t* tests corrected for multiple comparisons (*B*) or Mann–Whitney *U* (*C* and *D*): $*P < 0.05$, $**P < 0.01$, $***P < 0.001$. Abbreviations: Lck, lymphocyte-specific protein tyrosine kinase; pY, phosphotyrosine.

membrane integrity to assess the complex changes imparted by LXR on membrane lipids and order. Rather, we used pharmacological inhibitors of LXR (GSK2033) and UGCG (NB-DNJ). Inhibition of UCGG has been shown to attenuate proximal TCR signaling in Jurkat T cells, to reduce the production of IL-2 and IFNγ, and to inhibit proliferation (8, 52). Our own work also showed that inhibition of UGCG normalized T cell signaling and function in primary human T cells from SLE patients in vitro (7). We have also shown that in human T cells, increased glycosphingolipids are associated with increased accumulation of protein tyrosine phosphatase CD45 (which regulates Lck activity) within lipid rafts and increased Lck phosphorylation at the immune synapse (18). Thus, changes in lipid order and lipid profile could reflect an initial acceleration in signaling (seen as increased tyrosine phosphorylation), altered interaction between regulatory and inhibitory molecules, and altered downstream signaling events. This may not result in increased overall activation but result in changes in certain cytokine levels as we and others have described previously (39, 9, 53–58). Indeed, in T cells from SLE patients, inhibition of UGCG activity increased phosphorylation of TCRzeta and Erk yet dampened proliferation and proinflammatory cytokine production (7). Interestingly, Guy et al. (59) also demonstrated that cytokine production and proliferation can be uncoupled depending on the number of phosphorylated sites on the TCR subunits, whereby weak signals are sufficient to maintain cytokine production but fail to induce proliferation—similar to the phenotype observed here. Furthermore, changes in sphingolipid content at the immune synapse, specifically a decline in glucosylceramide (the product of UGCG), have been linked to T cell dysfunction in aged mice (60). Finally, reduced expression of the glycosphingolipid GM1 in effector T cells was associated with resistance to Treg suppression (61). Overall, these studies demonstrate that perturbation of UGCG activity and glycosphingolipid levels have been linked with abnormal TCR signaling at the immune synapse, resulting in altered effector functions. However, LXR had not previously been linked to glycosphingolipid metabolism.

It is important to note that changes in membrane lipid order, that could at first glance appear modest especially when compared with changes in gene expression, can nonetheless have important consequences in T cell function (9, 12, 62, 63). Changes in plasma membrane lipid order, measured using phase-sensitive probes, can affect T cell responses to TCR stimulation (9, 12). Specifically, high-order cells form a more stable immune synapse, resulting in a robust proliferative response and Th2 cytokine skew. In contrast, cells with lower order proliferate less and produce IFNγ (Th1) (9). Furthermore, pharmacologically reducing membrane order with an oxysterol is sufficient to alter the immune synapse between T cells and antigen-presenting cells and subsequent T cell proliferation and cytokine production (9, 10).

The discovery that LXR activation up-regulates UGCG expression in primary human immune cells provides a mode of action for LXR in the immune system. The magnitude of transcriptional activation by LXR, as for other nuclear receptors, depends on several factors, including chromatin architecture and epigenomic landscape at the specific gene that will determine cofactor recruitment and corepressor release or whether other signal-dependent transcription factors are present at the binding site (64). We observed that H3K27 acetylation at the UGCG site does not change in response to LXR ligand activation, similar to other LXR target genes (SMPDL3A is shown). This is not unusual for LXR regulation of gene expression (65). Changes in H3K27ac could be dynamic and altered with kinetics different to those of LXR binding. Additionally, other chromatin acetylation marks associated with transcriptional activation linked to gene activation in human CD4+ T cells or in the regulation of lipid metabolism could be relevant (66, 67). Future investigations will aim to characterize currently lacking global profiles of activation marks in these cells in response to LXR agonist and lipid changes. Furthermore, gene regulation may be mediated by the binding of additional signal-dependent transcription factors to adjacent sites (66). Finally, we and others have demonstrated that LXR regulation can be gene selective (68, 69).

UGCG is a ubiquitously expressed and highly conserved gene. To date, no post translational modifications have been identified, and transcriptional regulation appears to be the main determinant

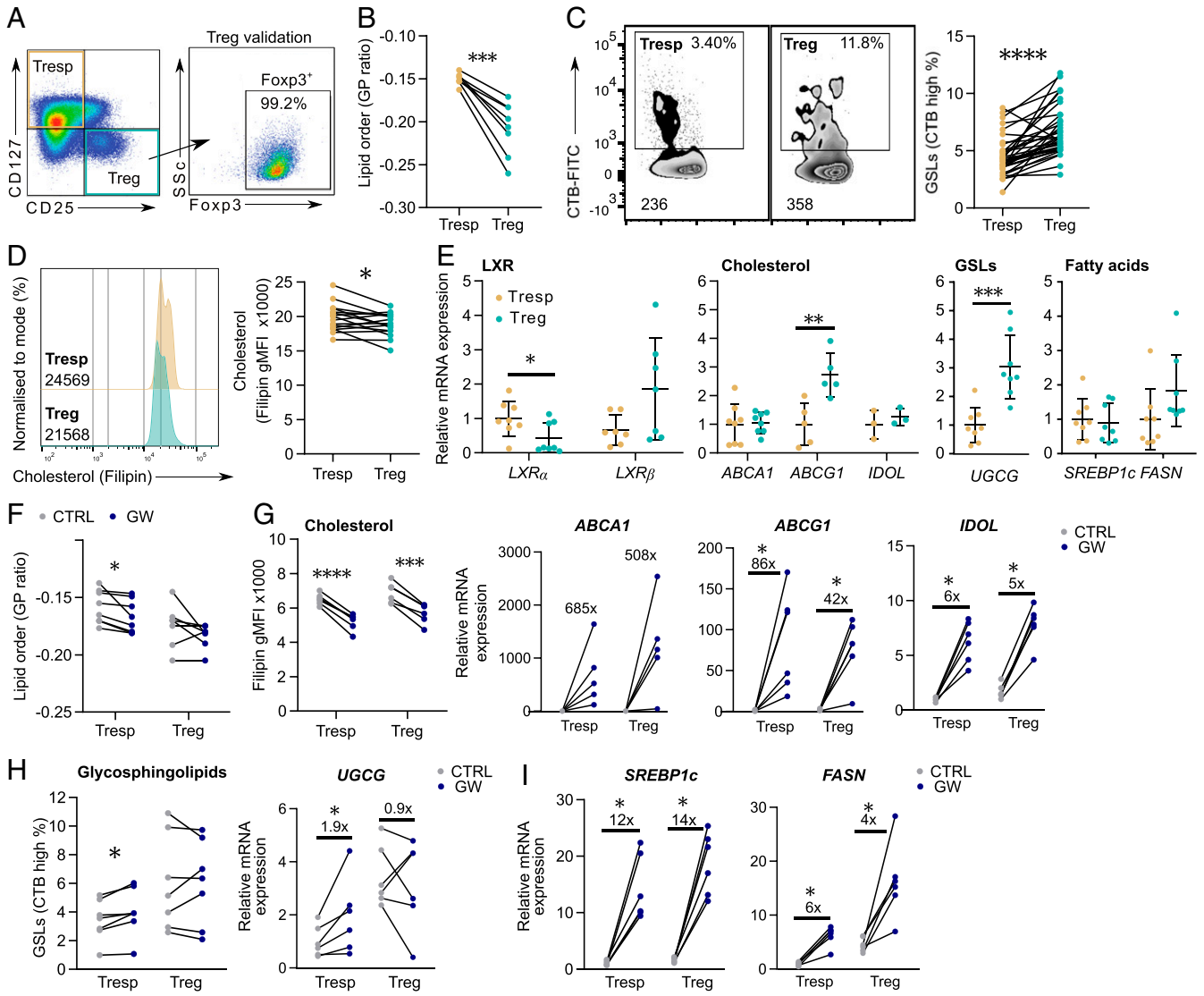

Fig. 6. Treg and Tresponder subsets have distinct lipid metabolic phenotypes. (*A*) Responder (Tresp: $CD4^+CD25^{lo}CD127^+$) and regulatory (Treg: $CD4^+CD25^+CD127^-$) T cell subsets were defined by flow cytometry. (*B–D*) Plasma membrane lipid order (GP ratio) (*B*), glycosphingolipid levels (GSL) (*C*), and cholesterol content (*D*) were analyzed using flow cytometry. Lines connect matched Tresp and Treg results from the same sample. (*E*) Expression of LXR- and LXR target genes that regulate cholesterol, GSL, and fatty acid levels were analyzed in FACS-sorted T cell subsets (n = 3-8). Mean ± SD. (*F–I*) Cells were treated with GW for 24 h. Lines connect CTRL- and GW-treated samples from the same donor. Cumulative data from three independent experiments show the change in membrane lipid order (GP ratio) (*F*), cholesterol (*G*), and GSL (*H*) expression. (*G–I*) Induction of LXR target genes involved in cholesterol (*G*), GSL (*H*), and fatty acid metabolism (*I*) were analyzed in FACS-sorted T cell subsets (n = 5 to 6). Gene expression is expressed relative to the average of CTRL-treated Tresp. The average fold change (GW versus CTRL) was calculated for each subset. Two-tailed t tests; $^*P < 0.05$, $^{**}P < 0.01$, $^{***}P < 0.001$, $^{****}P < 0.0001$.

of its activity (70). UGCG expression has been shown to be strongly up-regulated by a variety of inflammatory signals (71–74), in response to inhibition of prenylation by statin treatment (71–74), and by mTORC2 during tumorigenesis (75). It will be important to establish whether LXR-mediated regulation of UGCG extends to other cell types and tissues, as this could have wide-reaching implications for the therapeutic activation of LXR in various contexts. For example, elevated expression of UGCG has repeatedly been linked to acquisition of multidrug resistance and resistance to apoptosis in cancer models (76, 77). More recently, UGCG overexpression was shown to drive enhanced glutamine and mitochondrial metabolism in breast cancer cells (78–80).

LXR activation can be pro- or antiinflammatory depending on the timing of stimulation and species studied (43, 47, 48). LXR activation has previously been reported to inhibit cytokine production by T cells (38, 81, 82), generally attributed to repression of cytokine mRNA transcription (38, 81), which we did not observe here. We confirmed inhibition of proliferation and IL-17 production as previously observed (4, 38, 81, 82). However, we detected an increase in the production of both IL-2 and IL-4 and, in contrast to previous studies, did not observe inhibition of IFN-γ or TNF-α. Because the antiinflammatory actions of LXR are context dependent (29, 43, 48), it is likely that differences in the conditions for T cell or LXR activation could explain this discrepancy. For example, LXR activation can reduce production of IL-2, TNFα, and IFNγ in human $CD4^+$ T cells (81). However, in that study, T cells were only briefly stimulated with anti-CD3/28 (6 h), compared with long-term (72 h) exposure in our study. Furthermore, a different LXR ligand was used (T0901317), which has also been shown to act on other nuclear receptors (83). This suggests T0901317 activation could have led to LXR-independent effects on T cell function which would differ from those observed with a

more specific ligand such as GW. In addition, the timing, duration, and strength of stimulus as well as age and sex of donors can all influence LXR signaling (84, 85). Future studies could explore whether these factors are relevant in the LXR-dependent regulation of T cells. In our studies, LXR activation by GW did not significantly alter the induction of cytokine mRNA expression. Instead, the most significantly regulated transcriptional pathways were related to lipid metabolism, and we observed changes in plasma membrane lipid expression early (minutes) and late (72 h) in the course of T cell activation.

We identified that LXR-regulated genes and lipids were differentially expressed in Tregs. Like other nuclear receptors, LXR function is orchestrated by a complex combination of factors as mentioned above. Such mechanisms could contribute to subset-specific and gene-specific regulation as we have observed in human T cell subsets and will require further investigation. In murine cells, LXR has been suggested to play a critical role in Treg function (50), increase Foxp3 expression, and promote Treg differentiation (86). In contrast, LXR activation was recently shown to decrease the frequency of a subset of T cells, intestinal RORγt$^+$ Tregs, but this was attributed to an indirect effect on myeloid cells (87). While there is currently no evidence of the regulation of Treg and Tresp subsets by LXR in humans, rodent studies point to the importance of LXRβ in murine T regs (50). In mouse macrophages, LXRα and LXRβ exert overlapping but also specific transcriptional activities (69), although it is currently not known whether this also occurs in other cell types. Future studies will be needed to carefully dissect the mechanisms underlying the cell and LXR isotype–specific mechanisms of UGCG regulation.

In any case, a potential interaction between LXR signaling, plasma membrane lipids, and Tregs has not yet been explored. Murine Tregs also have low membrane order, and genetic deletion of ceramide synthesizing enzyme *smpd1* increases the frequency and suppressive capacity of Tregs (88). This supports a relationship between ceramide metabolism (in which UGCG plays a key role), plasma membrane lipid order, and Treg function. Although plasma membrane cholesterol has been shown to play an important role in the differentiation of Tregs (89), increasing plasma membrane cholesterol was reported to have no effect on their suppressive function (90). In contrast, reduction of intracellular cholesterol by 25-hydroxycholesterol or statin treatment inhibited Treg proliferation and expression of the immune checkpoint receptor CTLA-4 (91). Together, this work supports the hypothesis that LXR could contribute to Treg function via modulation of plasma membrane lipid order.

In addition to the changes in cholesterol and glycosphingolipid metabolism explored here, TAG levels were also substantially up-regulated by LXR activation. Compared with conventional T cells, Tregs are lipid enriched and have increased TAG synthesis and a greater concentration of lipid droplets which serve as a fuel source and protect against lipotoxicity (92). Furthermore, TAG also promote IL-7–mediated memory CD8$^+$ T cell survival (93). Thus, the role of LXR-driven TAG biosynthesis in T cells also warrants further investigation, although this was beyond the scope of our current study.

In their resting state, T cells express low levels of endogenous LXR ligands (94). In our experiments, CYP27A1 was the only oxysterol-synthesizing enzyme consistently expressed in these cells. However, there is evidence that certain polarization conditions can lead to dramatic regulation of oxysterol synthesis and thus endogenous modulation of LXR signaling. For example, in vitro differentiated type 1 regulatory cells up-regulate 25-hydroxychoelsterol to limit IL-10 production (94). In contrast, Th17 cells up-regulate an enzyme that sulfates oxysterols (SULT2B1), thereby inactivating them as LXR ligands and driving preferential activation of RORγt instead of LXR (95). LXR also plays a unique role in a subset of IL-9–producing CD8$^+$ T cells (Tc9), in which cholesterol/oxysterol are tightly supressed to prevent transrepression of the *Il9* locus by LXR (95). Furthermore, changes in oxysterol availability have been documented in many diseases, including accumulation in atherosclerotic plaques (96), production in the tumor microenvironment (6), and reduced circulating levels in multiple sclerosis (97). Therefore, the mechanism described here could be of therapeutic relevance to disorders characterized by defects in T cell signaling and lipid metabolism. For example, in addition to altered oxysterol levels, multiple sclerosis patients are reported to have altered LXR signaling, cholesterol levels, and glycosphingolipid metabolism (96). However, whether plasma membrane lipid rafts contribute to immune cell dysfunction in multiple sclerosis is currently unknown.

In conclusion, our findings show that LXR regulates glycosphingolipid levels, which strongly impacts plasma membrane lipid composition and T cell function. This mechanism is likely to be complementary to others modes of LXR action, including the transcriptional regulation of certain cytokines (6, 38) and modulation of endoplasmic reticulum cholesterol content (4). However, this mechanism could be of therapeutic relevance to disorders characterized by defects in T cell signaling and metabolism, including autoimmune and neurodegenerative diseases, cardiovascular disease, and cancer.

Materials and Methods

Antibodies and Reagents. A detailed list of antibodies and reagents is included in *SI Appendix, Methods*.

Human Samples. A total 50 mL of peripheral blood was collected from healthy controls (HCs). Men and women aged 18 to 60 were recruited. Exclusion criteria included current illness/infection, statin treatment, pregnancy, breast-feeding, or vaccination within the past 3 mo. For RNA-seq and lipidomic analysis of T cells from HC (Fig. 1) blood, leukocyte cones were purchased from National Health Service Blood and Transplant. PBMCs were separated on Ficoll–Paque PLUS (GE Healthcare) using SepMate tubes (Stemcell Technologies). PBMCs were cryopreserved in liquid nitrogen until use. Ethical approvals for this work were obtained from the London – City & East Research Ethics Committee (reference 15-LO-2065), Yorkshire & The Humber – South Yorkshire Research Ethics Committee (reference 16/YH/0306), South Central – Hampshire B Research Ethics Committee (reference 18/SC/0323). All participants provided informed written consent.

Cell Subset Purification.

Fluorescence-activated cell sorting. CD3$^+$ T cells for lipidomics analysis were sorted by fluorescence-activated cell sorting (FACS). Cells were washed in magnetic-assisted cell sorting (MACS) buffer (phosphate-buffered saline [PBS] with 2% fetal bovine serum [FBS] [Labtech] and 1 mM ethylenediamine tetraacetic acid [Sigma]) before staining with antibodies against surface markers for 30 min. Sorting was performed on a BD FACSAria II.

MACS. CD4$^+$ T cells and CD19$^+$ B cells were negatively isolated using magnetic bead–based separation (EasySep, Stemcell Technologies). CD14$^+$ monocytes were positively selected (EasySep, Stemcell Technologies). Sample purities were similar to those reported by the manufacturer (95.1 ± 1.3% for negative selection and 97.6 ± 0.21% for positive selection). To obtain monocyte-derived macrophages, monocytes were plated in low-serum media (1% FBS) for 1 to 2 h in 12-well Nunc-coated plates (Thermo Fisher Scientific) to promote adherence, then cultured for 7 d in complete media (Roswell Park Memorial Institute 1640 culture medium [Sigma] supplemented with 10% heat-inactivated FBS (Labtech) and 20 μg/mL gentamycin (Sigma).

Cell Culture. Full details of cell culture conditions and reagents are in *SI Appendix, Methods*.

Culture with LXR ligands. PBMCs or purified T cells were treated with GW3965 (GW) $^{+/-}$ RXR agonist LG100268 (LG) or UGCG inhibitor *N*-Butyldeoxynojirimycin (NB-DNJ) or with oxysterols, 24S-hydroxycholesterol, and 24S,25-epoxycholesterol and compared with either vehicle or LXR antagonist GSK1440233 as control.

Functional assays. T cells were stimulated with anti-CD3 and anti-CD28. To measure intracellular cytokine production cells were additionally stimulated with phorbol 12-myristate 13-acetate, ionomycin, and GolgiPlug.

Lipidomics. CD3$^+$ T cells were sorted by FACS and plated at 5×10^6 mL into 12-well plates in complete media ($n = 4$). A total of 10 to 15×10^6 cells were treated with dimethyl sulfoxide (control [CTRL]) or GW3965 (GW, 1 μM) for 36 h and washed twice in PBS. Frozen cell pellets were shipped to Lipotype

GmbH (Dresden) for mass spectrometry–based lipid analysis as described (98) (*SI Appendix, Methods*). Lipidomics data has been deposited at Mendeley Data (30).

RNA-Seq and Analysis. $CD4^+$ T cells (3×10^6) were treated with GW3965 (GW, 2 μM) for 24 h. The LXR antagonist GSK1440233 (CTRL, 1 μM) was used as a control to suppress baseline endogenous LXR activity. For TCR stimulation, cells were transferred to anti-CD3/28 coated plates for the last 18 h. Total RNA was extracted using TRIzol reagent (Life Technologies) followed by DNA-free DNA Removal Kit (Invitrogen). RNA integrity was confirmed using Agilent's 2200 Tapestation. UCL Genomics (London) performed library preparation and sequencing (*SI Appendix, Methods*). RNA-seq files are available at Array Express: E-MTAB-9141 (22).

Analysis of Gene Expression. Gene expression was measured by qPCR, as in refs. 28 and 65. Primers were used at a final concentration of 100 nM. Sequences are provided in *SI Appendix*, Table S3.

Flow Cytometry. Flow cytometry staining was performed as previously described (7, 9) (*SI Appendix, Methods*).

Immunoblotting. Cells were lysed in radioimmunoprecipitation assay buffer, and immunoblotting was performed as previously described (28). Semi-quantitative analysis was conducted using the gel analysis module in ImageJ (NIH, RRID: SCR_003070).

Chromatin Immunoprecipitation. Detailed description can be found in *SI Appendix, Methods*.

Microscopy.

Immunostaining. $CD4^+$ T cells were incubated in antibody-coated chamber slides for 15 min at 37 °C, 5% CO_2 to facilitate synapse formation. Medium and nonadherent cells were discarded, and wells were washed gently with PBS before fixation (4% paraformaldehyde, 2% sucrose, 140 mM NaOH, and pH 7.2) for 20 min at room temperature (RT). Formaldehyde was quenched with two washes in 0.1 M ammonium chloride (Sigma-Aldrich), followed by a PBS wash. 0.2% Trition-X-100 was used to permeabilize cells for 8 min at RT. Samples were blocked with 5% bovine serum albumin in PBS + 0.2% fish skin gelatin (Sigma-Aldrich) overnight at 4 °C. Primary antibodies were added in blocking solution for 1 h at RT, followed by addition of fluorescently conjugated secondary antibodies for 30 min RT. Cells were preserved in Prolong Diamond mounting media with DAPI (Invitrogen). Fixed synapses were stained with phalloidin-fluorescein isothiocyanate conjugate (Sigma).

Confocal microscopy. Single slices were acquired on a Leica SPE2 confocal microscope with an ×63 oil-immersion objective and 488 and 633 nM excitation solid-state lasers, using the following settings: 1024 × 1024 pixels, 600 Hz, and line average of 3.

TIRF microscopy. To record live cells stained with di-4-ANEPPDHQ probe (ANE), a customized two-channel setup was used as described by Ashdown et al. (62) and in *SI Appendix, Methods*. In total, 30-min movies were acquired at a rate of 1 frame/minute. The background mean fluorescence identity (MFI) was based on three measurements taken from the area surrounding each cell.

Image analysis. Image analysis was performed using ImageJ 1.51 (IH, RRID: SCR_003070). Fluorescence intensity was analyzed using the "Analyze Particles" function. MFI was measured as mean gray scale value (between 0 and 255), and corrected total cell fluorescence (CTCF) was calculated as follows: CTCF = integrated density − (cell area × MFI of background). To analyze TIRF movies of ANE-stained cells, ordered and disordered channels were aligned using the Cairn Image Splitter plugin. Membrane lipid order was calculated as a GP ratio, using the plugin at https://github.com/quokka79/GPcalc (GitHub, RRID: SCR_002630). Hue, saturation, and brightness images were set to visualize GP and pseudocolored using the Rainbow RGB look-up table.

Statistical Analysis. Statistical tests were performed in GraphPad Prism 8 (GraphPad Software, La Jolla, California, RRID: SCR_002798, https://www.graphpad.com/) unless otherwise stated. The D'Agostino–Pearson omnibus K2 test was used to check whether datasets were normally distributed. In some cases, extreme outliers were removed based upon a robust regression and outlier removal test (Q = 1%). Unpaired two-tailed *t* tests or Mann–Whitney *U* were used to compare between independent groups and are represented as bar charts (mean ± SD) or violin plots (median and interquartile range). In line with previous studies on LXR agonism in human cells (7, 81, 99), paired two-tailed *t* tests or repeated measures ANOVA were used where cells from the same donor sample were exposed to different treatments (e.g., GW versus CTRL). This minimizes the impact of donor-to-donor heterogeneity at baseline. Where paired tests were applied, data are presented as paired line graphs. Correction for multiple comparisons was made with Tukey's post hoc test or Dunnet's test (to compare all samples with vehicle), as specified. For Fig. 5*B*, *P* values from multiple unpaired *t* test were corrected using the two-stage linear step-up procedure of Benjamini, Krieger, and Yekutieli with false discovery rate (FDR) threshold of 5%.

Data Availability. RNA-seq and Lipidomics data have been deposited in ArrayExpress (https://www.ebi.ac.uk/arrayexpress/experiments/E-MTAB-9141/) and Mendeley Data (DOI: 10.17632/5rzpnr7w65.1).

ACKNOWLEDGMENTS. We are grateful to K.R. Steffenson for the provision of the LXR antibody used for chromatin immunoprecipitation and to A. Castrillo and J. Thorne for earlier discussions on LXRE identification in the UGCG gene. K.E.W. was funded by a British Heart Foundation PhD Studentship (FS/13/59/30649) and the Multiple Sclerosis Society (Grant 76). I.P.-T. was funded by a Medical Research Council New Investigator Grant (G0801278), a British Heart Foundation Project Grant (PG/13/10/30000), and an Academy of Medical Sciences Newton Advanced Fellowship. E.C.J. was funded by Innovative Medicines Initiative Joint Grant Agreement No. 115303, as part of the Anti-Biopharmaceutical Immunization: Prediction and Analysis of Clinical Relevance to Minimize the Risk consortium; Arthritis Research UK Fellowships (20085 and 18106); Lupus United Kingdom; The Rosetrees Trust (Grant M409); and the University College London Hospital Clinical Research and Development Committee (Project Grant GCT/2008/EJ and Fast Track Grant F193).

1. K. Simons, E. Ikonen, Functional rafts in cell membranes. *Nature* **387**, 569–572 (1997).
2. M. Swamy *et al*., A cholesterol-based allostery model of T cell receptor phosphorylation. *Immunity* **44**, 1091–1101 (2016).
3. F. Wang, K. Beck-García, C. Zorzin, W. W. A. Schamel, M. M. Davis, Inhibition of T cell receptor signaling by cholesterol sulfate, a naturally occurring derivative of membrane cholesterol. *Nat. Immunol.* **17**, 844–850 (2016).
4. S. J. Bensinger *et al*., LXR signaling couples sterol metabolism to proliferation in the acquired immune response. *Cell* **134**, 97–111 (2008).
5. Y. Kidani *et al*., Sterol regulatory element-binding proteins are essential for the metabolic programming of effector T cells and adaptive immunity. *Nat. Immunol.* **14**, 489–499 (2013).
6. X. Ma *et al*., Cholesterol negatively regulates IL-9-producing $CD8^+$ T cell differentiation and antitumor activity. *J. Exp. Med.* **215**, 1555–1569 (2018).
7. G. McDonald *et al*., Normalizing glycosphingolipids restores function in CD4+ T cells from lupus patients. *J. Clin. Invest.* **124**, 712–724 (2014).
8. Y. Zhu *et al*., Lowering glycosphingolipid levels in CD4+ T cells attenuates T cell receptor signaling, cytokine production, and differentiation to the Th17 lineage. *J. Biol. Chem.* **286**, 14787–14794 (2011).
9. L. Miguel *et al*., Primary human CD4+ T cells have diverse levels of membrane lipid order that correlate with their function. *J. Immunol.* **186**, 3505–3516 (2011).
10. D. M. Owen *et al*., High plasma membrane lipid order imaged at the immunological synapse periphery in live T cells. *Mol. Membr. Biol.* **27**, 178–189 (2010).
11. K. Simons, E. Ikonen, How cells handle cholesterol. *Science* **290**, 1721–1726 (2000).
12. K. Gaus, E. Chklovskaia, B. Fazekas de St Groth, W. Jessup, T. Harder, Condensation of the plasma membrane at the site of T lymphocyte activation. *J. Cell Biol.* **171**, 121–131 (2005).
13. C. Rentero *et al*., Functional implications of plasma membrane condensation for T cell activation. *PLoS One* **3**, e2262 (2008).
14. W. Wu, X. Shi, C. Xu, Regulation of T cell signalling by membrane lipids. *Nat. Rev. Immunol.* **16**, 690–701 (2016).
15. W. Yang *et al*., Potentiating the antitumour response of CD8(+) T cells by modulating cholesterol metabolism. *Nature* **531**, 651–655 (2016).
16. D. Sviridov, N. Mukhamedova, Y. I. Miller, Lipid rafts as a therapeutic target. *J. Lipid Res.* **61**, 687–695 (2020).
17. N. S. Heaton, G. Randall, Multifaceted roles for lipids in viral infection. *Trends Microbiol.* **19**, 368–375 (2011).
18. E. C. Jury, P. S. Kabouridis, F. Flores-Borja, R. A. Mageed, D. A. Isenberg, Altered lipid raft-associated signaling and ganglioside expression in T lymphocytes from patients with systemic lupus erythematosus. *J. Clin. Invest.* **113**, 1176–1187 (2004).
19. E. C. Jury, D. A. Isenberg, C. Mauri, M. R. Ehrenstein, Atorvastatin restores Lck expression and lipid raft-associated signaling in T cells from patients with systemic lupus erythematosus. *J. Immunol.* **177**, 7416–7422 (2006).
20. B. Wang, P. Tontonoz, Liver X receptors in lipid signalling and membrane homeostasis. *Nat. Rev. Endocrinol.* **14**, 452–463 (2018).
21. J. L. Collins *et al*., Identification of a nonsteroidal liver X receptor agonist through parallel array synthesis of tertiary amines. *J. Med. Chem.* **45**, 1963–1966 (2002).
22. K. E. Waddington, E. C. Jury, I. Pineda-Torra, E-MTAB-9141 - RNA-seq of primary human CD4+ T cells treated with the LXR agonist GW3965, with and without TCR stimulation. Array Express EMBL-EBI. https://www.ebi.ac.uk/arrayexpress/experiments/E-MTAB-9141/. Deposited 30 December 2020.
23. A. C. Calkin, P. Tontonoz, Transcriptional integration of metabolism by the nuclear sterol-activated receptors LXR and FXR. *Nat. Rev. Mol. Cell Biol.* **13**, 213–224 (2012).

24. J. N. Benhammou *et al*., Novel lipid long intervening noncoding RNA, oligodendrocyte maturation-associated long intergenic noncoding RNA, regulates the liver steatosis gene stearoyl-coenzyme A desaturase as an enhancer RNA. *Hepatol. Commun.* **3**, 1356–1372 (2019).
25. E. A. DiBlasio-Smith *et al*., Discovery and implementation of transcriptional biomarkers of synthetic LXR agonists in peripheral blood cells. *J. Transl. Med.* **6**, 59 (2008).
26. B. A. Laffitte *et al*., Autoregulation of the human liver X receptor alpha promoter. *Mol. Cell. Biol.* **21**, 7558–7568 (2001).
27. E. D. Muse *et al*., Cell-specific discrimination of desmosterol and desmosterol mimetics confers selective regulation of LXR and SREBP in macrophages. *Proc. Natl. Acad. Sci. U.S.A.* **115**, E4680–E4689 (2018).
28. M. C. Gage *et al*., Disrupting LXRα phosphorylation promotes FoxM1 expression and modulates atherosclerosis by inducing macrophage proliferation. *Proc. Natl. Acad. Sci. U.S.A.* **115**, E6556–E6565 (2018).
29. K. E. Waddington, E. C. Jury, I. Pineda-Torra, Liver X receptors in immune cell function in humans. *Biochem. Soc. Trans.* **43**, 752–757 (2015).
30. K. E. Waddington, G. E. Robinson, I. Pineda-Torra, E. C. Jury, Lipidomics analysis of primary human T cells after LXR activation with GW3965. Mendeley Data. https://doi.org/10.17632/5rzpnr7w65.1. Deposited 1 September 2020.
31. K. R. Levental *et al*., Polyunsaturated lipids regulate membrane domain stability by tuning membrane order. *Biophys. J.* **110**, 1800–1810 (2016).
32. E. Sezgin, I. Levental, S. Mayor, C. Eggeling, The mystery of membrane organization: Composition, regulation and roles of lipid rafts. *Nat. Rev. Mol. Cell Biol.* **18**, 361–374 (2017).
33. A. F. Valledor *et al*., Activation of liver X receptors and retinoid X receptors prevents bacterial-induced macrophage apoptosis. *Proc. Natl. Acad. Sci. U.S.A.* **101**, 17813–17818 (2004).
34. B. A. Laffitte *et al*., The phospholipid transfer protein gene is a liver X receptor target expressed by macrophages in atherosclerotic lesions. *Mol. Cell. Biol.* **23**, 2182–2191 (2003).
35. P. Pehkonen *et al*., Genome-wide landscape of liver X receptor chromatin binding and gene regulation in human macrophages. *BMC Genomics* **13**, 50 (2012).
36. I. Lavrnja *et al*., Expression profiles of cholesterol metabolism-related genes are altered during development of experimental autoimmune encephalomyelitis in the rat spinal cord. *Sci. Rep.* **7**, 2702 (2017).
37. P. B. Noto *et al*., Regulation of sphingomyelin phosphodiesterase acid-like 3A gene (SMPDL3A) by liver X receptors. *Mol. Pharmacol.* **82**, 719–727 (2012).
38. G. Cui *et al*., Liver X receptor (LXR) mediates negative regulation of mouse and human Th17 differentiation. *J. Clin. Invest.* **121**, 658–670 (2011).
39. D. Lingwood, K. Simons, Lipid rafts as a membrane-organizing principle. *Science* **327**, 46–50 (2010).
40. R. Varma, G. Campi, T. Yokosuka, T. Saito, M. L. Dustin, T cell receptor-proximal signals are sustained in peripheral microclusters and terminated in the central supramolecular activation cluster. *Immunity* **25**, 117–127 (2006).
41. F. Bovenga, C. Sabbà, A. Moschetta, Uncoupling nuclear receptor LXR and cholesterol metabolism in cancer. *Cell Metab.* **21**, 517–526 (2015).
42. K. Mouzat *et al*., Regulation of brain cholesterol: What role do liver X receptors play in neurodegenerative diseases? *Int. J. Mol. Sci.* **20**, 3858 (2019).
43. C. Fontaine *et al*., Liver X receptor activation potentiates the lipopolysaccharide response in human macrophages. *Circ. Res.* **101**, 40–49 (2007).
44. S. Ghisletti *et al*., Parallel SUMOylation-dependent pathways mediate gene- and signal-specific transrepression by LXRs and PPARgamma. *Mol. Cell* **25**, 57–70 (2007).
45. A. Ito *et al*., LXRs link metabolism to inflammation through Abca1-dependent regulation of membrane composition and TLR signaling. *eLife* **4**, e08009 (2015).
46. X. Rong *et al*., LXRs regulate ER stress and inflammation through dynamic modulation of membrane phospholipid composition. *Cell Metab.* **18**, 685–697 (2013).
47. Y. Sohrabi *et al*., LXR activation induces a proinflammatory trained innate immunity-phenotype in human monocytes. *Front. Immunol.* **11**, 353 (2020).
48. M. Ishibashi *et al*., Liver x receptor regulates arachidonic acid distribution and eicosanoid release in human macrophages: A key role for lysophosphatidylcholine acyltransferase 3. *Arterioscler. Thromb. Vasc. Biol.* **33**, 1171–1179 (2013).
49. C. T. Chan *et al*., Liver X receptors are required for thymic resilience and T cell output. *J. Exp. Med.* **217**, e20200318 (2020).
50. A. J. Michaels, C. Campbell, R. Bou-Puerto, A. Y. Rudensky, Nuclear receptor LXRβ controls fitness and functionality of activated T cells. *J. Exp. Med.* **218**, e20201311 (2020).
51. J. M. Carbó *et al*., Pharmacological activation of LXR alters the expression profile of tumor-associated macrophages and the abundance of regulatory T cells in the tumor microenvironment. *Cancer Res.* **81**, 968–985 (2021).
52. N. Blank, M. Schiller, C. Gabler, J. R. Kalden, H. M. Lorenz, Inhibition of sphingolipid synthesis impairs cellular activation, cytokine production and proliferation in human lymphocytes. *Biochem. Pharmacol.* **71**, 126–135 (2005).
53. I. Gombos, E. Kiss, C. Detre, G. László, J. Matkó, Cholesterol and sphingolipids as lipid organizers of the immune cells' plasma membrane: Their impact on the functions of MHC molecules, effector T-lymphocytes and T-cell death. *Immunol. Lett.* **104**, 59–69 (2006).
54. P. S. Kabouridis, E. C. Jury, Lipid rafts and T-lymphocyte function: Implications for autoimmunity. *FEBS Lett.* **582**, 3711–3718 (2008).
55. R. A. Maldonado, D. J. Irvine, R. Schreiber, L. H. Glimcher, A role for the immunological synapse in lineage commitment of CD4 lymphocytes. *Nature* **431**, 527–532 (2004).
56. F. Balamuth, D. Leitenberg, J. Unternaehrer, I. Mellman, K. Bottomly, Distinct patterns of membrane microdomain partitioning in Th1 and th2 cells. *Immunity* **15**, 729–738 (2001).
57. E. Izsepi *et al*., Membrane microdomain organization, calcium signal, and NFAT activation as an important axis in polarized Th cell function. *Cytometry A* **83**, 185–196 (2013).
58. M. V. Farrell, S. Webster, K. Gaus, J. Goyette, T cell membrane heterogeneity aids antigen recognition and T cell activation. *Front. Cell Dev. Biol.* **8**, 609 (2020).
59. C. S. Guy *et al*., Distinct TCR signaling pathways drive proliferation and cytokine production in T cells. *Nat. Immunol.* **14**, 262–270 (2013).
60. A. Molano *et al*., Age-dependent changes in the sphingolipid composition of mouse CD4+ T cell membranes and immune synapses implicate glucosylceramides in age-related T cell dysfunction. *PLoS One* **7**, e47650 (2012).
61. G. Wu, Z. H. Lu, H. J. Gabius, R. W. Ledeen, D. Bleich, Ganglioside GM1 deficiency in effector T cells from NOD mice induces resistance to regulatory T-cell suppression. *Diabetes* **60**, 2341–2349 (2011).
62. G. W. Ashdown *et al*., Membrane lipid order of sub-synaptic T cell vesicles correlates with their dynamics and function. *Traffic* **19**, 29–35 (2018).
63. T. Zech *et al*., Accumulation of raft lipids in T-cell plasma membrane domains engaged in TCR signalling. *EMBO J.* **28**, 466–476 (2009).
64. Z. Czimmerer, L. Halasz, L. Nagy, Unorthodox transcriptional mechanisms of lipid-sensing nuclear receptors in macrophages: Are we opening a new chapter? *Front. Endocrinol. (Lausanne)* **11**, 609099 (2020).
65. N. Becares *et al*., Impaired LXRα phosphorylation attenuates progression of fatty liver disease. *Cell Rep.* **26**, 984–995.e6 (2019).
66. Q. Zhang *et al*., MS-275 induces hepatic FGF21 expression via H3K18ac-mediated CREBH signal. *J. Mol. Endocrinol.* **62**, 187–196 (2019).
67. Z. L. Cui *et al*., Histone modifications of Notch1 promoter affect lung CD4+ T cell differentiation in asthmatic rats. *Int. J. Immunopathol. Pharmacol.* **26**, 371–381 (2013).
68. N. Becares, M. C. Gage, I. Pineda-Torra, Posttranslational modifications of lipid-activated nuclear receptors: Focus on metabolism. *Endocrinology* **158**, 213–225 (2017).
69. A. Ramón-Vázquez *et al*., Common and differential transcriptional actions of nuclear receptors liver X receptors α and β in macrophages. *Mol. Cell. Biol.* **39**, e00376-18 (2019).
70. Y. Ishibashi, A. Kohyama-Koganeya, Y. Hirabayashi, New insights on glucosylated lipids: Metabolism and functions. *Biochimic. Biophys. Acta* **1831**, 1475–1485 (2013).
71. M. S. Köberlin *et al*., A conserved circular Network of coregulated lipids modulates innate immune responses. *Cell* **162**, 170–183 (2015).
72. P. J. Brennan *et al*., Invariant natural killer T cells recognize lipid self antigen induced by microbial danger signals. *Nat. Immunol.* **12**, 1202–1211 (2011).
73. M. K. Pandey *et al*., Complement drives glucosylceramide accumulation and tissue inflammation in Gaucher disease. *Nature* **543**, 108–112 (2017).
74. A. K. Iyer, J. Liu, R. M. Gallo, M. H. Kaplan, R. R. Brutkiewicz, STAT3 promotes CD1d-mediated lipid antigen presentation by regulating a critical gene in glycosphingolipid biosynthesis. *Immunology* **146**, 444–455 (2015).
75. B. Binnington *et al*., Inhibition of Rab prenylation by statins induces cellular glycosphingolipid remodeling. *Glycobiology* **26**, 166–180 (2016).
76. M. W. Khan *et al*., mTORC2 controls cancer cell survival by modulating gluconeogenesis. *Cell Death Discov.* **1**, 15016 (2015).
77. Y. Guri *et al*., mTORC2 promotes tumorigenesis via lipid synthesis. *Cancer Cell* **32**, 807–823.e12 (2017).
78. Y. Y. Liu, R. A. Hill, Y. T. Li, Ceramide glycosylation catalyzed by glucosylceramide synthase and cancer drug resistance. *Adv. Cancer Res.* **117**, 59–89 (2013).
79. Y. Lavie, H. Cao, S. L. Bursten, A. E. Giuliano, M. C. Cabot, Accumulation of glucosylceramides in multidrug-resistant cancer cells. *J. Biol. Chem.* **271**, 19530–19536 (1996).
80. M. S. Wegner *et al*., UDP-glucose ceramide glucosyltransferase activates AKT, promoted proliferation, and doxorubicin resistance in breast cancer cells. *Cell. Mol. Life Sci.* **75**, 3393–3410 (2018).
81. D. Walcher *et al*., LXR activation reduces proinflammatory cytokine expression in human CD4-positive lymphocytes. *Arterioscler. Thromb. Vasc. Biol.* **26**, 1022–1028 (2006).
82. L. Wu *et al*., Activation of the liver X receptor inhibits Th17 and Th1 responses in Behcet's disease and Vogt-Koyanagi-Harada disease. *Curr. Mol. Med.* **14**, 712–722 (2014).
83. K. A. Houck *et al*., T0901317 is a dual LXR/FXR agonist. *Mol. Genet. Metab.* **83**, 184–187 (2004).
84. S. Della Torre *et al*., An essential role for liver ERα in coupling hepatic metabolism to the reproductive cycle. *Cell Rep.* **15**, 360–371 (2016).
85. K. Y. DeLeon-Pennell *et al*., LXR/RXR signaling and neutrophil phenotype following myocardial infarction classify sex differences in remodeling. *Basic Res. Cardiol.* **113**, 40 (2018).
86. M. Herold *et al*., Liver X receptor activation promotes differentiation of regulatory T cells. *PLoS One* **12**, e0184985 (2017).
87. S. M. Parigi *et al*., Liver X receptor regulates Th17 and RORγt(+) Treg cells by distinct mechanisms. *Mucosal Immunol.* **14**, 411–419 (2021).
88. C. Hollmann *et al*., Inhibition of acid sphingomyelinase allows for selective targeting of CD4+ conventional versus Foxp3+ regulatory T cells. *J. Immunol.* **197**, 3130–3141 (2016).
89. H. Y. Cheng *et al*., Loss of ABCG1 influences regulatory T cell differentiation and atherosclerosis. *J. Clin. Invest.* **126**, 3236–3246 (2016).
90. J. Surls *et al*., Increased membrane cholesterol in lymphocytes diverts T-cells toward an inflammatory response. *PLoS One* **7**, e38733 (2012).
91. H. Zeng *et al*., mTORC1 couples immune signals and metabolic programming to establish T(reg)-cell function. *Nature* **499**, 485–490 (2013).
92. D. Howie *et al*., A novel role for triglyceride metabolism in Foxp3 expression. *Front. Immunol.* **10**, 1860 (2019).
93. G. Cui *et al*., IL-7-Induced glycerol transport and TAG synthesis promotes memory CD8+ T cell longevity. *Cell* **161**, 750–761 (2015).
94. S. Vigne *et al*., IL-27-Induced type 1 regulatory T-cells produce oxysterols that constrain IL-10 production. *Front. Immunol.* **8**, 1184 (2017).
95. X. Hu *et al*., Sterol metabolism controls T(H)17 differentiation by generating endogenous RORγ agonists. *Nat. Chem. Biol.* **11**, 141–147 (2015).
96. N. J. Spann *et al*., Regulated accumulation of desmosterol integrates macrophage lipid metabolism and inflammatory responses. *Cell* **151**, 138–152 (2012).
97. K. Fellows Maxwell *et al*., Oxysterols and apolipoproteins in multiple sclerosis: A 5 year follow-up study. *J. Lipid Res.* **60**, 1190–1198 (2019).
98. J. L. Sampaio *et al*., Membrane lipidome of an epithelial cell line. *Proc. Natl. Acad. Sci. U.S.A.* **108**, 1903–1907 (2011).
99. D. L. Asquith *et al*., The liver X receptor pathway is highly upregulated in rheumatoid arthritis synovial macrophages and potentiates TLR-driven cytokine release. *Ann. Rheum. Dis.* **72**, 2024–2031 (2013).